Hydrometallurgy 138 (2013) 1–13

Contents lists available at SciVerse ScienceDirect

Hydrometallurgy

journal homepage: www.elsevier.com/locate/hydromet

Effect of Na-chloride on the bioleaching of a chalcopyrite concentrate in shake flasks and stirred tank bioreactors ☆

Denise Bevilaqua [a,b,*], Heidi Lahti [a], Patrícia H. Suegama [c], Oswaldo Garcia Jr. [a,b,1], Assis V. Benedetti [b], Jaakko A. Puhakka [a], Olli H. Tuovinen [a,d]

[a] Department of Chemistry and Bioengineering, Tampere University of Technology, P.O. Box 541, FI-33101 Tampere, Finland
[b] Institute of Chemistry, UNESP, Univ. Estadual Paulista, Araraquara, SP CEP 14.901-970, Brazil
[c] Departamento de Química, Universidade Federal da Grande Dourados, Dourados, MS, CEP 79.825-070, Brazil
[d] Department of Microbiology, Ohio State University, 484 West 12th Avenue, Columbus, OH 43210, USA

ARTICLE INFO

Article history:
Received 11 September 2012
Received in revised form 28 May 2013
Accepted 17 June 2013
Available online 27 June 2013

Keywords:
Acidithiobacillus
Bioleaching
Chloride
Chalcopyrite
Electrochemical analysis

ABSTRACT

Oxidative dissolution of chalcopyrite at ambient temperatures is generally slow and subject to passivation, posing a major challenge for developing bioleaching applications for this recalcitrant mineral. Chloride is known to enhance the chemical leaching of chalcopyrite, but much of this effect has been demonstrated at elevated temperatures. This study was undertaken to test whether 100–200 mM Na-chloride enhances the chemical and bacterial leaching of chalcopyrite in shake flasks and stirred tank bioreactor conditions at mesophilic temperatures. *Acidithiobacillus ferrooxidans*, *Acidithiobacillus thiooxidans* and abiotic controls were employed for the leaching experiments. Addition of Na-chloride to the bioleaching suspension inhibited the formation of secondary phases from chalcopyrite and decreased the Fe(III) precipitation. Neither elemental S nor secondary Cu-sulfides were detected in solid residues by X-ray diffraction. Chalcopyrite leaching was enhanced when the solution contained bacteria, ferrous iron and Na-chloride under low redox potential (<450 mV) conditions. Scanning electron micrographs and energy-dispersive analysis of X-rays revealed the presence of precipitates that were identified as brushite and jarosites in solid residues. Minor amounts of gypsum may also have been present. Electrochemical analysis of solid residues was in concurrence of the differential effects between chemical controls, chloride ions, and bacteria. Electrochemical impedance spectroscopy was used to characterize interfacial changes on chalcopyrite surface caused by different bioleaching conditions. In abiotic controls, the impedance signal stabilized after 28 days, indicating the lack of changes on mineral surface thereafter, but with more resistive behavior than chalcopyrite itself. For bioleached samples, the signal suggested some capacitive response with time owing to the formation of less conductive precipitates. At Bode-phase angle plots (middle frequency), a new time constant was observed that was associated with the formation of jarosite, possibly also with minor amount or elemental S, although this intermediate could not be verified by XRD. Real impedance vs. frequency plots indicated that the bioleaching continued to modify the chalcopyrite/solution interface even after 42 days.

1. Introduction

Chalcopyrite ($CuFeS_2$) is a primary Cu-sulfide of considerable interest in biohydrometallurgy because it is abundant but refractory and its bioleaching at ambient temperatures is subject to surface passivation. Several studies of chalcopyrite leaching with chloride-based solutions have been published over the years (e.g., Al-Harahsheh et al., 2008; Carneiro and Leão, 2007; Kinnunen et al., 2004; Sato et al., 2000), and they show that chalcopyrite leaching rates with Fe(III)-chloride are faster than with Fe(III)-sulfate. This effect has been related to the formation of a more porous sulfur layer as a secondary phase in the presence of chloride (Liang et al., 2012; Lu et al., 2000) and thus larger areas for reactant diffusion and contact with reactive surface of chalcopyrite. The formation of Cu-chloride complexes and enhanced redox potential are also possible causes for the faster leaching rates (Carneiro and Leão, 2007). Copper is monovalent in the chalcopyrite structure and its dissolution could increase with the formation of soluble Cu^{+}–Cl^{-} complexes. Cai et al. (2012) detected a secondary, Cl-containing covellite (CuS) phase that hindered chalcopyrite dissolution in chloride leaching. Both chalcocite (Cu_2S) and covellite have been detected on chalcopyrite surface in

* Corresponding author at: Departamento de Bioquímica e Tecnologia Química, Instituto de Química de Araraquara, Universidade Estadual Paulista, Araraquara, SP, CEP 14.901-970, Brazil. Tel.: +55 16 33019677; fax: +55 16 33222308.
E-mail address: denise@iq.unesp.br (D. Bevilaqua).
[1] Deceased.

0304-386X/$ – see front matter © 2013 The Authors. Published by Elsevier B.V. All rights reserved.
http://dx.doi.org/10.1016/j.hydromet.2013.06.008

sulfate-rich bioleaching experiments (e.g., Ahmadi et al., 2011; He et al., 2012; Xia et al., 2010).

The effect of chloride on acid leaching of chalcopyrite has been quite widely studied, whereas the chloride effect on the bioleaching has gained less attention. On one hand, chloride has been reported to enhance chemical and biological leaching of chalcopyrite (Kinnunen et al., 2004; Ruiz et al., 2012; Yoo et al., 2010). On other hand, elevated chloride levels in leach solutions are inhibitory to iron and sulfur oxidizing microorganisms (Gahan et al., 2009, 2010; Xiong and Guo, 2011; Zammit et al., 2012). Shiers et al. (2005) reported that the ability of mesophilic iron-oxidizers to adapt to chloride was limited. However, chloride-tolerant iron-oxidizing acidophiles have now been shown to exist (Davis-Belmar et al., 2008; Wang et al., 2012; Zammit et al., 2012). Published information shows differences in chloride toxicity to bioleaching microorganisms. For example, Gahan et al. (2009) found that chloride at 4 g/l (110 mM) was lethal to a pyrite-oxidizing microbial consortium that comprised Fe-oxidizers, S-oxidizers and archaea. Deveci et al. (2008) reported that salinity in the range of 1–4% NaCl w/v (170–680 mM NaCl) was increasingly detrimental to mesophilic bioleaching microorganisms. Harahuc et al. (2000) reported that iron oxidation by washed cells of iron-grown *Acidithiobacillus ferrooxidans* was partially inhibited already at 10 mM KCl, but sulfur-grown cells oxidized iron in the presence of up to 200 mM of chloride. In fact, slight enhancement of sulfur oxidation in the presence of 50 mM KCl was reported and active oxidation of sulfur in the presence of 400 mM KCl was still measurable.

Elemental sulfur formation contributes to the passivation layer in chalcopyrite leaching (Klauber, 2008; Watling, 2006). Lu et al. (2000) reported that the presence of chloride ion increased the crystallinity and porosity of the sulfur formed during chalcopyrite leaching, giving better access for the oxidant to the mineral surface. In the absence of chloride, chalcopyrite became coated by a poorly crystallized film of sulfur, which may have hindered the leaching. Carneiro and Leão (2007) determined the surface area and porosity of leach residues in the presence and absence of Na-chloride at 95 °C. The surface area and porosity of secondary solid phases increased during chalcopyrite leaching with 0.5–2.0 M Na-chloride in the leach solution. Liang et al. (2012) reported that 11 mM sodium Na-chloride greatly decreased the amount of elemental S accumulation during thermophilic bioleaching (65 °C) of chalcopyrite.

The purpose of this study was to characterize the effect of chloride on the bioleaching of a chalcopyrite concentrate in the range of 100–200 mM Na-chloride. In an effort to define conditions for enhanced Cu leaching from chalcopyrite, various combinations of iron- and sulfur-oxidizing bacteria were used with Na-chloride, coupled with analyses of solid residues by X-ray diffraction for mineralogical changes and electrochemical studies to examine changes in semiconductor and charge transfer properties of chalcopyrite.

2. Materials and methods

2.1. Bacteria and growth conditions

Acidithiobacillus ferrooxidans LR and *Acidithiobacillus thiooxidans* FG01 (Garcia, 1991) were used in this study. The cultures were grown in mineral salts medium (MSM) which contained (per liter) 0.5 g each of $(NH_4)_2SO_4$, K_2HPO_4, and $MgSO_4 \cdot 7H_2O$. Trace metals were added (mg/l) as $FeCl_3 \cdot 6H_2O$ (11.0), $CuSO_4 \cdot 5H_2O$ (0.5), H_3BO_3 (2.0), $MnSO_4 \cdot H_2O$ (2.0), $Na_2MoO_4 \cdot 2H_2O$ (0.8), $CoCl_2 \cdot 6H_2O$ (0.6), $ZnSO_4 \cdot 7H_2O$ (0.9), and Na_2SeO_4 (0.1), pH 1.8 (Dopson and Lindström, 1999; Kaksonen et al., 2011). *A. ferrooxidans* was grown with 6.6 g Fe^{2+}/l, added as 120 mM $FeSO_4 \cdot 7H_2O$ and sufficient to increase cell yields to $>10^8$ cells/ml (Tuovinen and Kelly, 1973). The trace metals and ferrous sulfate were sterilized as separate stock solutions by membrane filtration (0.45 μm). *A. ferrooxidans* LR was previously also adapted to grow with 2.5% chalcopyrite (Bevilaqua et al., 2002). *A. ferrooxidans* also grows with elemental S (S^0) but it was not used as a substrate for this bacterium in the present study. *A. thiooxidans* was grown with 10 g S^0/l. Sulfur was dry sterilized at 150 °C for 24 h. Aseptic techniques were used in handling, inoculation and sampling of the cultures. The cultures were incubated at 26 ± 2 °C and at 150 rpm on a rotatory shaker and transferred in fresh media with 10% inocula. Cell counts were not determined in the experiments because of the uncertainty of distribution of attached and planktonic cells during chalcopyrite oxidation. As an approximation, the inoculation of Fe^{2+}-grown *A. ferrooxidans* yielded initial concentrations of the low range of 10^7 cells/ml in chalcopyrite cultures in shake flasks.

2.2. Chloride experiments on chalcopyrite bioleaching in shake flasks

The chalcopyrite concentrate sample used in this study was obtained from Vale SA (Rio de Janeiro, Brazil). The concentrate was ground to 100% −200 mesh (74 μm opening). The bulk concentrate contained 23.0% Cu, 27.3% Fe, 22.9% S, 3.2% Si and 7.0% Ca and comprised chalcopyrite as the only sulfide phase and minor amounts of quartz, hydroxylapatite and hornblende. The bacteria used in this experiment were chalcopyrite-adapted *A. ferrooxidans* and S^0-grown *A. thiooxidans*. The pulp density was 2.5%. The culture media were adjusted to initial pH 1.6 with H_2SO_4. Duplicate 150 ml suspensions in 250 ml shake flasks were incubated at 26 ± 2 °C and at 150 rpm. Evaporation was compensated for with sterile deionized water. The effect of Na-chloride ion on the bioleaching of the chalcopyrite concentrate sample was studied in shake flasks under several different conditions (Table 1).

2.3. Stirred tank bioreactor leaching experiments with chalcopyrite

Leaching of chalcopyrite (2.5% pulp density) was tested in three bioreactor runs with a total liquid volume of 1.5 l and 10% inoculum of *A. ferrooxidans* or *A. thiooxidans*. The design of the baffled bioreactor is shown in Fig. 1. The bioreactor leaching conditions are specified in Table 2 and they included the addition of 100 mM Na-chloride initially (runs 1 and 2) or after 15 days (run 3) and bacterial inoculation initially (*A. ferrooxidans*), after 9 days (*A. thiooxidans*), or 15 days (*A. ferrooxidans*). The time course of bioreactor leaching was extended to 45 (runs 1 and 2) and 58 days (run 3). The additions were partly chosen on the basis of the shake flask results except in run 3, where the purpose was to test the effect of 100 mM Na-chloride after four weeks of contact time (midway through the time course). The bioreactor leaching was started at initial

Table 1
Test conditions used in Na-chloride shake flask leaching experiments with 2.5% chalcopyrite in MSM and the summary of XRD analyses. All conditions included MSM as the base leach solution.

Set	Experimental conditions	Designation[a]
1	*A. ferrooxidans* + 100 mM Na-chloride	Cl + *Af*
2[b]	100 mM Na-chloride; *A. ferrooxidans* inoculum added on 15	Cl + *Af*(15d)
3	100 mM Na-chloride + *A. ferrooxidans*; another aliquot of 100 mM Na-chloride added on day 15	Cl + *Af* + Cl(15d)
4[c]	100 mM Na-chloride + *A. ferrooxidans*; *A. thiooxidans* inoculum added on day 15	Cl + *Af* + *At*(15d)
5	CuFeS2 adapted *A. ferrooxidans;* no Na-chloride	*Af*
6	100 mM Na-chloride; another aliquot of 100 mM Na-chloride added on day 15 (chemical control)	Cl + Cl(15d)
7	100 mM Na-chloride (chemical control)	Cl
8	MSM only (no Na-chloride, no bacteria; chemical control)	Control
9	Spent *A. ferrooxidans* medium (120 mM Fe3+) + 100 mM Na-chloride	Oxidized + Cl
10	*A. thiooxidans*; no Na-chloride	*At*

[a] *Af* = *A. ferrooxidans*; *At* = *A. thiooxidans*; Cl = 100 mM Na-chloride.
[b] Set 2: This was designed to test whether the inoculation of *A. ferrooxidans* after 15 days of chemical leaching with Na-chloride could enhance the leaching.
[c] Set 4: *A. thiooxidans* inoculum was added after 15 days in an effort to enhance the oxidation of intermediate sulfur in the event that elemental S would otherwise accumulate.

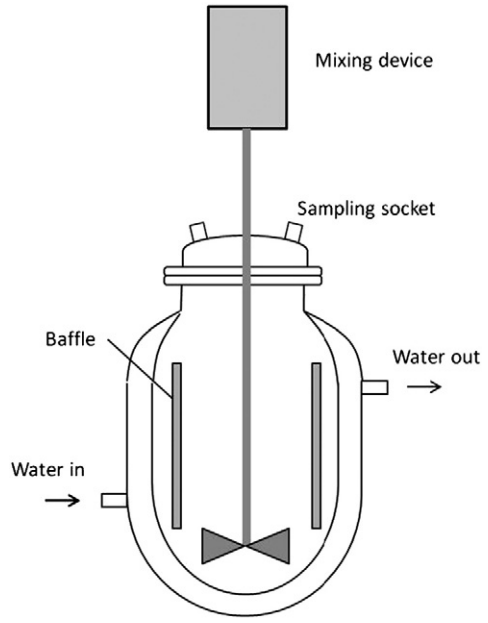

Fig. 1. Design of the bioreactor used in this study.

pH 1.6 for each run to accommodate the increases in pH, which were controlled with manual addition of H_2SO_4 during the experiments to keep the pH < 2.5. Temperature was held constant at 28 ± 2 °C with a water bath. The bioreactors were aerated with 1.5 l air/min and stirred at 180 rpm. Evaporation was compensated for with sterile deionized water. The time course in each experiment was extended based on the cumulative dissolution of Cu.

2.4. Analytical methods

Shake flasks were periodically sampled (4 ml) for pH and redox potential (Ag/AgCl/KCl reference) measurements. For chemical and X-ray diffraction (XRD) analysis, the sample volume was increased to 15 ml. Samples for the chemical analyses were centrifuged samples (10,000 *g* for 15 min) and the concentration of Fe^{2+} was determined with the *o*-phenanthroline method (American Public Health Association et al., 1998). Aliquots of supernatants were preserved in 1 M HCl for analysis of dissolved Cu and total dissolved Fe by atomic absorption spectrometry. The concentration of Fe^{3+} was calculated from the total Fe and Fe^{2+} data. Solid residues were washed with dilute H_2SO_4 (adjusted to the same pH as the culture suspension; pH 1.6–2.0) three times before drying in air at 26 °C, followed by storage under Ar headspace. The mineralogical composition was analyzed by XRD (Siemens D-500) equipped with a diffracted-beam monochromator and CuKα radiation. Samples were scanned from 10 to 70°2θ at 0.05°2θ increments with 2 s counting time.

Table 2
Test conditions used in Na-chloride leaching experiments with 2.5% chalcopyrite in bioreactors. All conditions included MSM as the base leach solution.

Run	Experimental conditions	Designation
1	100 mM Na-chloride; *A. ferrooxidans* inoculum added on day 15	Cl + *Af*(15d)
2	100 mM Na-chloride + *A. ferrooxidans*; *A. thiooxidans* inoculum added on day 9	Cl + *Af* + *At*(15d)
3	*A. ferrooxidans*; 100 mM Na-chloride added on day 15	*Af* + *Cl(15d)*

Af = *A. ferrooxidans*; *At* = *A. thiooxidans*; Cl = 100 mM Na-chloride.

2.5. Electrochemical measurements

Samples of leach residues for the electrochemical analysis were chosen from shake flask experiments 1, 5, 7 and 8 (Table 1). The residues were used to prepare carbon paste-modified electrodes (CPE) as previously described (Bevilaqua et al., 2009). A total powder mixture containing 0.4 g of graphite (Aldrich), 0.1 g of chalcopyrite leach residue (<400 mesh) and 0.075 g of mineral oil (Nujol) was mixed with chloroform to obtain a homogenous paste which was preserved under O_2-free atmosphere. The paste was placed in a cavity on the electrode body, in contact with a 7.5 mm^2 Pt-disk with a geometric area of 7.10 mm^2 to be exposed to the solution. For electrochemical analysis an Ag|AgCl|KCl_{sat} assembly, connected to the solution through a Luggin capillary, was used as reference electrode. A Pt-wire was used as the auxiliary electrode and the CPE-residues were the working electrodes.

Electrochemical impedance spectroscopy measurements of the CPE-residues were performed using a Reference 600 Gamry potentiostat, equipped with a three-electrode electrochemical cell and CPE-chalcopyrite as working electrode. A Pt-disk electrode connected to the reference by a 10 μF capacitor was used to minimize the noise at low frequency range and the phase shift at high frequency region (Mansfeld et al., 1988). The impedance spectra were obtained by applying on the open circuit potential value a small root mean square amplitude potential wave (10 mV). The frequency range was varied from 100 kHz to 5 mHz, recording 10 points per frequency decade.

The results of the electrochemical measurements were used to calculate the Nyquist and Bode plots. When a sinusoidal potential or current perturbation with certain frequency is applied to an electrode/solution interface, the response will be a sinusoidal current or potential signal with the same frequency. The ac potential/ac current ratio (i.e., the resistance to current flow in an ac circuit) is the impedance (Z), defined at a particular frequency ω as

$$Z(\omega) = Z_{real} + jZ_{imag},$$

where Z_{real} and Z_{imag} are the real and imaginary parts of impedance, respectively, and j = imaginary unit satisfying $\sqrt{-1}$ (i.e., $j^2 = -1$). The Z_{real} is frequency independent, and the Z_{imag} is frequency dependent. The imaginary impedance ($-Z_{imag}$) vs. the real impedance (Z_{real}) gives the Nyquist plot. This is a complex plane where each point is read at selected frequency defined by the frequency interval and the numbers of points/frequency decade are defined in the experimental setup. Frequencies do not appear explicitly. If the system responds as a pure resistance, both the perturbation and response signals are in-phase and the imaginary impedance Z_{imag} is zero. If the system behaves as a pure capacitor, the Nyquist plot is a series of impedance values positioned on the Z_{imag} axis and inversely proportional with the frequency; the real part of impedance Z_{real} is zero. If the system has an inductive behavior, the impedance behaves similarly to the capacitor, but the impedance is directly proportional to the frequency. In both cases, the response signal is out-of-phase with the perturbation signal, by a negative or positive phase angle Φ. The modulus of impedance |Z| is related with both real and imaginary impedance by $|Z| = (Z_{real}^2 + Z_{imag}^2)^{1/2}$. The impedance data can also be represented by Bode plots, in which the modulus of impedance as log |Z| or the phase angle Φ is plotted versus log f, where f is the frequency in Hz. The phase angle and modulus of impedance are related with the real and imaginary impedance by $Z_{real} = |Z|\cos\Phi$ and $Z_{imag} = |Z|\sin\Phi$ and the phase angle is defined as $\Phi = \tan^{-1}(Z_{imag}/Z_{real})$.

3. Results

3.1. Chalcopyrite leaching experiments in shake flasks

The effect of Na-chloride on chalcopyrite bioleaching was examined by using Na-chloride in different combinations with *A. ferrooxidans* and

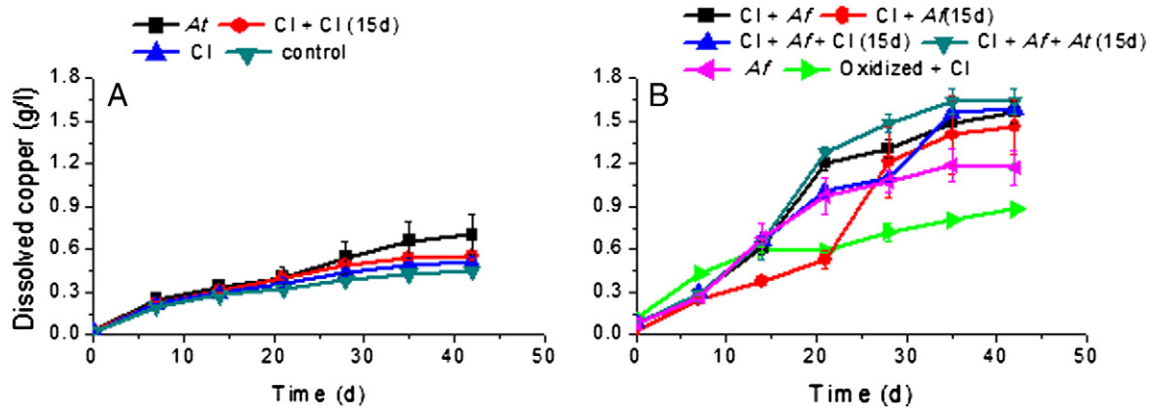

Fig. 2. Changes in dissolved copper concentration from chalcopyrite in shake flasks. A, chemical controls (Sets 6, 7, 8, and 10) and *A. thiooxidans* culture (Set 10); B, *A. ferrooxidans* cultures (Sets 1 through 5 and 9). See Table 1 for specific experimental details.

A. thiooxidans cultures and abiotic controls. The results showed that 100 mM Na-chloride had a negligible effect on copper dissolution in abiotic controls (Fig. 2). Chalcopyrite leaching with *A. thiooxidans* resulted in slightly elevated copper dissolution, which was attributed to sulfur oxidation to sulfuric acid. The yield of Cu leaching by *A. thiooxidans* was low as compared to the bioleaching of Cu in *A. ferrooxidans* cultures.

Copper dissolution decreased with time in the presence of Na-chloride and *A. ferrooxidans*, and a similar trend was observed in spent medium. The highest extent of copper dissolution was obtained with 100 mM Na-chloride and *A. ferrooxidans* combination that received an additional *A. thiooxidans* inoculum on day 15. Time courses of copper dissolution in other cultures with Na-chloride displayed similar patterns of gradual rate decline. These data suggested that hindered dissolution of copper was caused by surface passivation of chalcopyrite, which may be caused by precipitation of jarosite and/or formation of secondary solid phases during chalcopyrite oxidation such as CuS or S^0. This phenomenon, chalcopyrite passivation, has been previously reported in numerous bioleaching studies (e.g., Ahmadi et al., 2011; Sasaki et al., 2009; Watling, 2006; Xia et al., 2010).

The corresponding changes in Fe^{2+}, Fe^{3+} and total dissolved Fe concentrations are shown in Figs. 3 and 4. Although no Fe was added in the mineral salts media, total dissolved Fe concentration was about 180 mg/l within a matter of hours and increased to about 200 mg Fe/l after 7 days of contact with *A. thiooxidans*-inoculated leach solution (Fig. 3). In the absence of Na-chloride, the concentrations of Fe remained low in abiotic controls and in *A. ferrooxidans* cultures (Fig. 3). In cultures containing Na-chloride and bacterial inocula, the concentration of dissolved Fe increased, whereas the level of Fe^{2+} remained

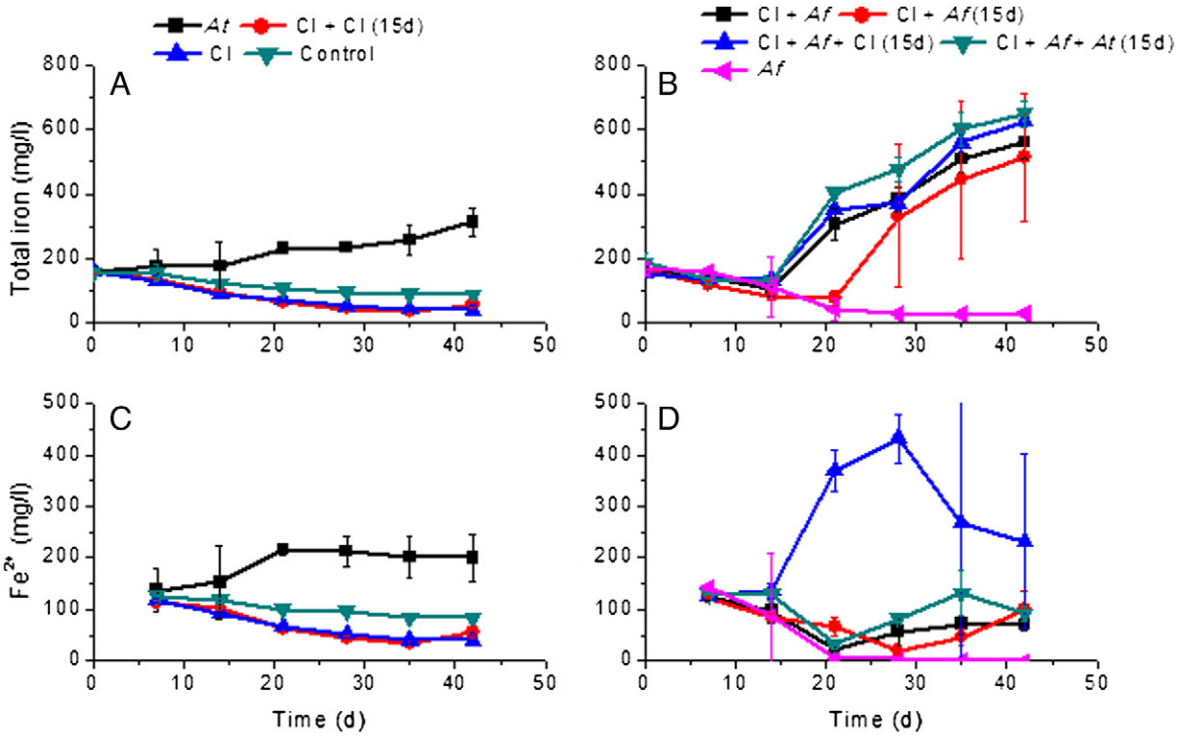

Fig. 3. Changes in dissolved iron concentration during chalcopyrite leaching in shake flasks. A and C, total iron and ferrous iron concentrations in chemical controls (Sets 6, 7, 8, and 10) and *A. thiooxidans* culture (Set 10); B and D, total iron and ferrous iron concentrations in *A. ferrooxidans* cultures (Sets 1 through 5 and 9). See Table 1 for specific experimental details.

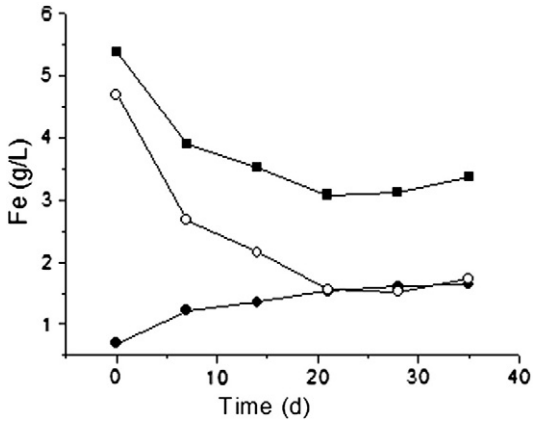

Fig. 4. Changes in the total iron (■), Fe^{3+} (○), and Fe^{2+} (●) concentration in the presence of 100 mM Na-chloride during chalcopyrite bioleaching by *A. ferrooxidans*.

low (Fig. 3). It is possible that stabilization of dissolved ferric iron complexes with chloride ion decreased Fe(III)-precipitation, thus contributing to the increase in dissolved Fe.

As shown in Fig. 4, the total Fe decreased with time in the presence of 100 M Na-chloride while the concentration of Fe^{2+} remained relatively low. This trend is taken to represent continuing oxidation of Fe^{2+} by *A. ferrooxidans* and precipitation of Fe^{3+} most likely as a jarosite type mineral. The medium contained 100 mM Na^+ as well as minor amounts of K^+ (5.7 mM) and NH_4^+ (7.6), which would result in the precipitation of jarosite as a solid solution comprised of hydronium, potassium, ammonium, and sodium jarosites.

Additional Na-chloride on day 15 inhibited the bacterial oxidation, seen as an increase in Fe^{2+} concentration (Fig. 3). This culture subsequently commenced Fe^{2+} oxidation after a two week delay. Similarly, a lag period preceding iron oxidation was also observed in the combination of 120 mM Fe^{2+}, 2.5% chalcopyrite and 100 mM Na-chloride in inoculated medium. The lag period was attributed to increased inhibition of *A. ferrooxidans* caused by the salinity, seen as an increase in Fe^{2+} concentration and prolongation of low redox potential phase (Figs. 3 and 5).

The results also showed that the dissolved Fe concentration increased in parallel with redox potential (Fig. 3). The pH values in the Na-chloride-containing abiotic controls increased over 20 days of contact in leach solution. In the inoculated flasks the pH values started to decrease after 2 weeks, indicating acid formation. Oxidation of the S entity of $CuFeS_2$ is an acid-forming reaction but it was not measured in this study. The decrease in pH was not a direct result of ferric iron hydrolysis and precipitation because the concentration of dissolved Fe continued to increase. Fe(III) precipitation was evident in abiotic controls that included 100 mM Na-chloride.

Fig. 6 shows the time course of Cu dissolution when 100 mM Na-chloride was added to *A. ferroxidans* culture on day 44. Cu-dissolution was slightly enhanced whereas in the parallel reference culture (no Na-chloride addition) Cu-dissolution continued at a declining rate, which was attributed to passivation of chalcopyrite surface. As the dissolved Cu data were not immediately available due to analytical delay, the experiment was terminated before the two curves were resolved better.

3.2. Chalcopyrite leaching in stirred tank bioreactors

Three bioreactor runs were conducted at 2.5% pulp density of the chalcopyrite concentrate: run 1) MSM with 100 mM Na-chloride and inoculation of *A. ferrooxidans* after 15 days of contact time; run 2) MSM with 100 mM Na-chloride and *A. ferrooxidans*, with inoculation of *A. thiooxidans* after 9 days of contact time; and run 3) MSM with *A. ferrooxidans* and addition of 100 mM Na-chloride after 28 days of contact time. The results are presented in Fig. 7. The pH values in the bioreactor that included *A. ferrooxidans* and 100 mM Na-chloride (run 1) increased over time although the culture was daily adjusted to pH 2.5. Addition of *A. thiooxidans* on day 9 to the bioreactor that contained

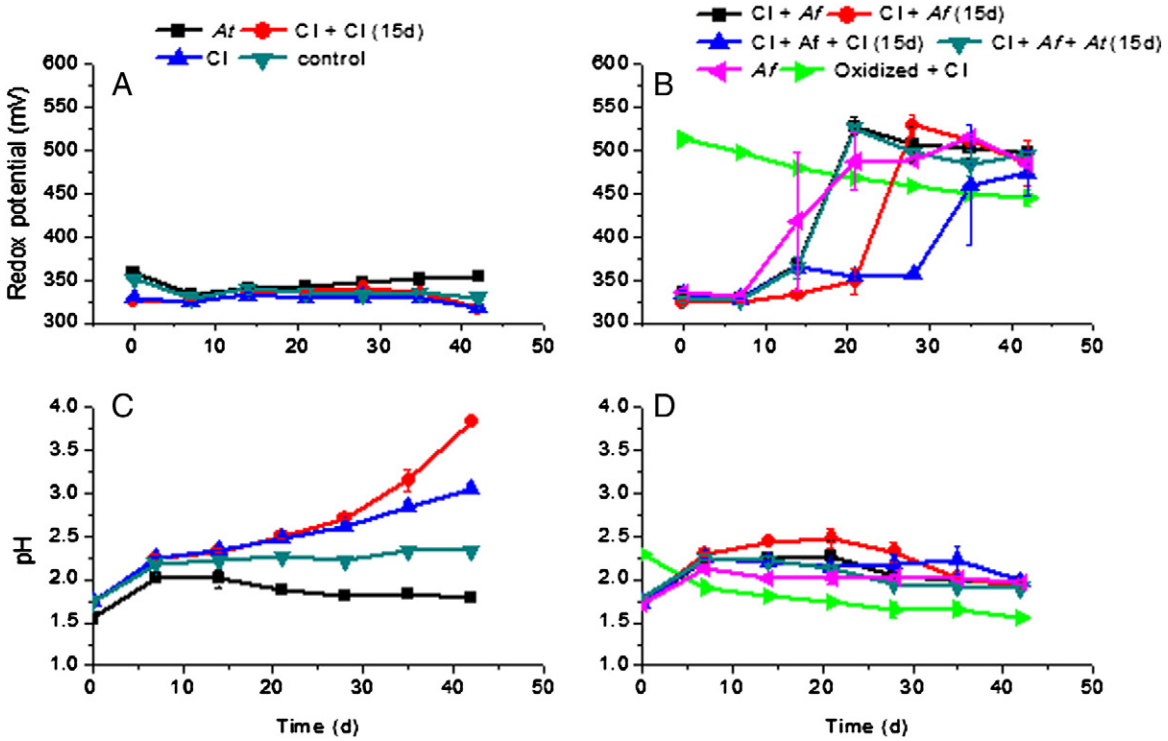

Fig. 5. Changes in redox potential and pH during chalcopyrite leaching in shake flasks. A and C, chemical controls (Sets 6, 7, 8, and 10) and *A. thiooxidans* culture (Set 10); B and D, *A. ferrooxidans* cultures (Sets 1 through 5 and 9). See Table 1 for specific experimental details.

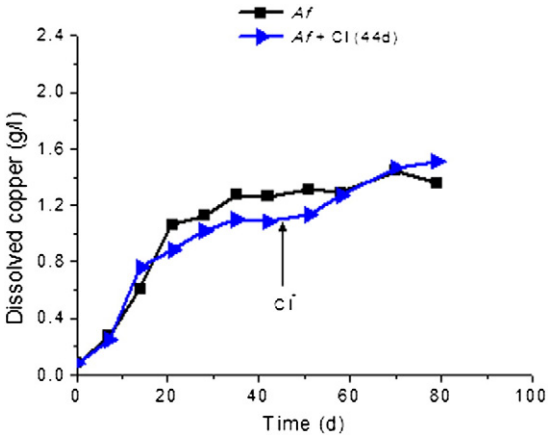

Fig. 6. Changes in copper concentration during chalcopyrite leaching by *A. ferrooxidans* after 100 mM Na-chloride addition into a duplicate flask on day 44.

A. ferrooxidans and 100 mM Na-chloride (run 2) controlled the increasing pH only slightly, but subsequently the concentration of dissolved Fe started to increase. In run 3 with *A. ferrooxidans*, the dissolved iron concentration increased after the addition of 100 mM Na-chloride on day 28. The concentrations of Fe^{2+} remained low in all bioreactor experiments. The redox potentials and yields of copper leaching remained lower in run 1, which initially contained 100 mM Na-chloride, than in runs 2 and 3. The results also showed that Na-chloride addition transiently decreased the redox potential, perhaps because of the inhibition of ferrous iron oxidation caused by Na-chloride. Because of the NaCl addition, the midpoint of the redox potential may have been lowered by ferric iron-chloride complexes but further thermodynamic analysis was not within the scope of this study. The inhibition of the oxidation of the S-entity and intermediates may also be involved.

3.3. XRD analysis of solid residues

Chalcopyrite dissolution by bacterial leaching usually yields elemental S, typically as a sulfur rim on the mineral grains as part of the passivation effect, and its further oxidation to sulfate is relatively slow even in the presence of sulfur-oxidizing acidithiobacilli (Klauber, 2008; Watling, 2006). Possible reasons for slow elemental S oxidation include tenacity and the lack of porosity of the elemental S layer, constraining bacterial access to solid substratum (He et al., 2012; Rodríguez et al., 2003). Intermediate elemental S may not be detectable by XRD because, as an approximation, XRD detection level of crystallized phases is about 2% in solid samples depending on the mineralogical composition, sample matrix and instrumentation. Several studies have reported the lack of XRD detection of elemental S in chalcopyrite leach residues

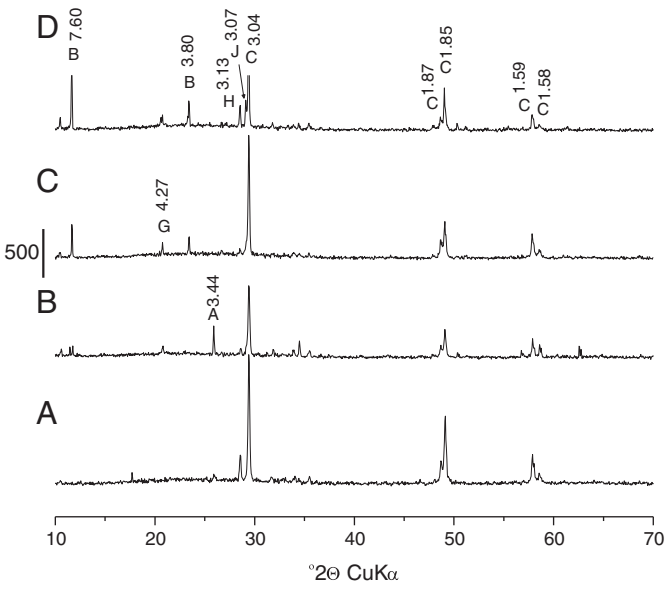

Fig. 8. X-ray diffractograms of (A) untreated chalcopyrite and solids after (B) 28 days, (C) 42 days, and (D) 58 days of contact in *A. ferrooxidans* culture. Letter designations and PDF numbers: A = hydroxylapatite (01-089-6440), B = brushite (00-011-0293), C = chalcopyrite (00-037-0471), G = gypsum (00-033-0311), H = hornblende (00-045-1371), and J = jarosite (00-036-0427). The vertical bar shows the relative scale of counts. The *d*-values are given in Ångströms.

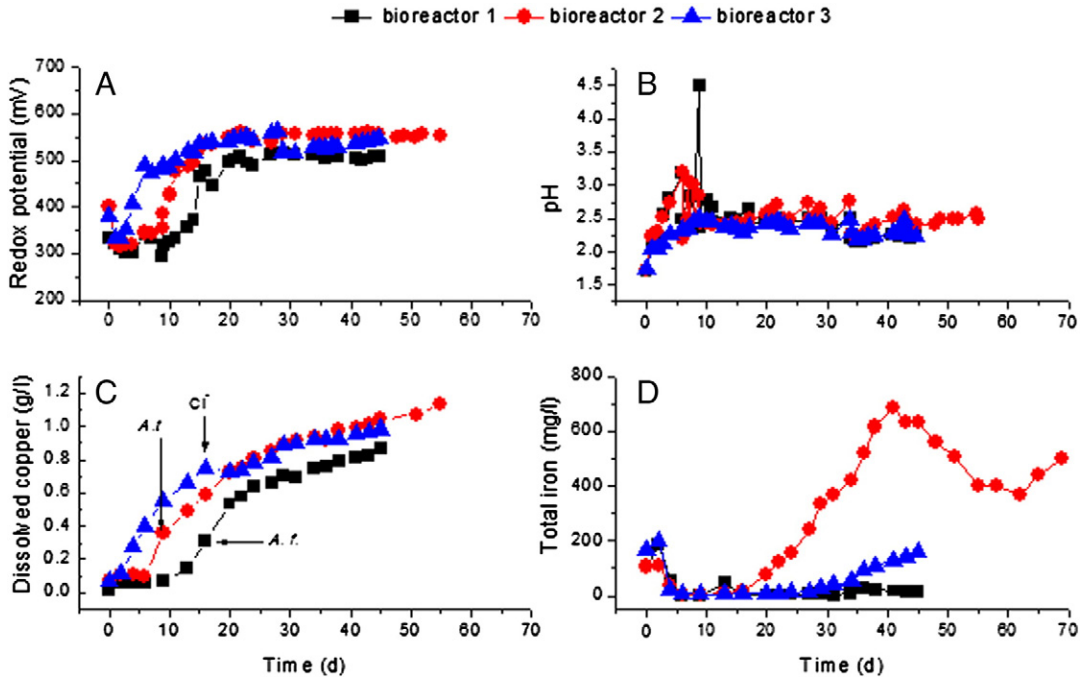

Fig. 7. Changes in redox potential (A), pH (B), and concentration of dissolved copper (C) and total iron (D) during chalcopyrite leaching in the bioreactor experiment (Run 1).

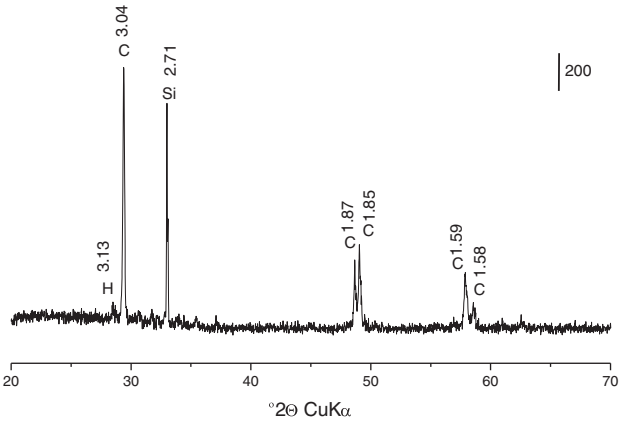

Fig. 9. X-ray diffractogram of solid residues after 14 days of contact with *A. ferrooxidans* and 100 mM Na-chloride. Letter designations: C = chalcopyrite and H = hornblende. The peak labeled Si is from silica wafer in the sample holder. The vertical bar shows the relative scale of counts. The *d*-values are given in Ångströms.

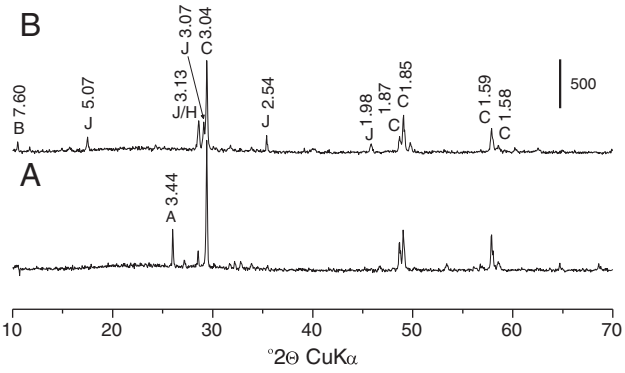

Fig. 11. X-ray diffractograms of solid residues from chalcopyrite leaching experiments after 58 days of contact. A, *A. ferrooxidans* with 100 mM Na-chloride, inoculated with *A. thiooxidans* after 15 days; B, spent medium of *A. ferrooxidans* with 100 mM Na-chloride. Letter designations: A = hydroxylapatite, B = brushite, C = chalcopyrite, G = gypsum, H = hornblende, and J = jarosite. The vertical bar shows the relative scale of counts. The *d*-values are given in Ångströms.

(e.g., Fu et al., 2008; Liang et al., 2012; Zhou et al., 2007). Jarosite type minerals are also common components in chalcopyrite passivation layer in mesophilic and thermophilic bioleaching of chalcopyrite (Fu et al., 2008; He et al., 2009, 2012; Panda et al., 2013; Xia et al., 2010). Secondary Cu-sulfides have also been found in passivation layers during chalcopyrite bioleaching (Klauber, 2008; Sasaki et al., 2009; Watling, 2006; Zeng et al., 2013).

Fig. 8 presents X-ray patterns of an untreated chalcopyrite sample and solids after 28, 42 and 58 days of leaching with *A. ferrooxidans* in shake flasks. The untreated sample contained chalcopyrite as the major phase ($d = 3.04$ Å) and minor amounts of hornblende ($d = 3.13$ Å) and hydroxylapatite ($d = 3.44$ Å), the peak possibly overlapping with quartz. Other peaks could not be identified with certainty because of their low relative intensity in the baseline. The solids after 28 days of contact with *A. ferrooxidans* culture contained chalcopyrite, hornblende and quartz. Gypsum ($CaSO4{\cdot}2H_2O$; $d = 4.27$ Å) was identified as a secondary phase. After 42 days of contact, gypsum and brushite ($CaPO_3(OH){\cdot}2H_2O$; $d = 7.60$ Å) were the main secondary phases. Additionally, a minor phase of jarosite was detected in 58 day samples. The main peak assigned to a jarosite type mineral was a shoulder ($d = 3.07$ Å) because it was partly masked by the main peak of chalcopyrite ($d = 3.04$ Å). Other peaks of the minor jarosite phase cannot be discerned from the baseline in Fig. 8. The solubilization of the minor impurity, hydroxylapatite, is believed to be the source gypsum and brushite.

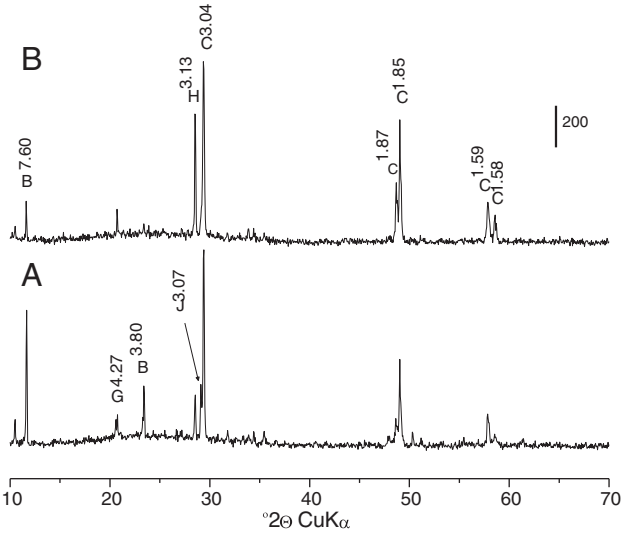

Fig. 10. X-ray diffractograms of solid residues from chalcopyrite bioleaching after 58 days of contact with *A. ferrooxidans*. A, Solids from *A. ferrooxidans* culture (no Na-chloride); B, solids from *A. ferrooxidans* culture, with 100 mM Na-chloride added on day 44. Letter designations: B = brushite, C = chalcopyrite, G = gypsum, H = hornblende, and J = jarosite. The vertical bar shows the relative scale of counts. The *d*-values are given in Ångströms.

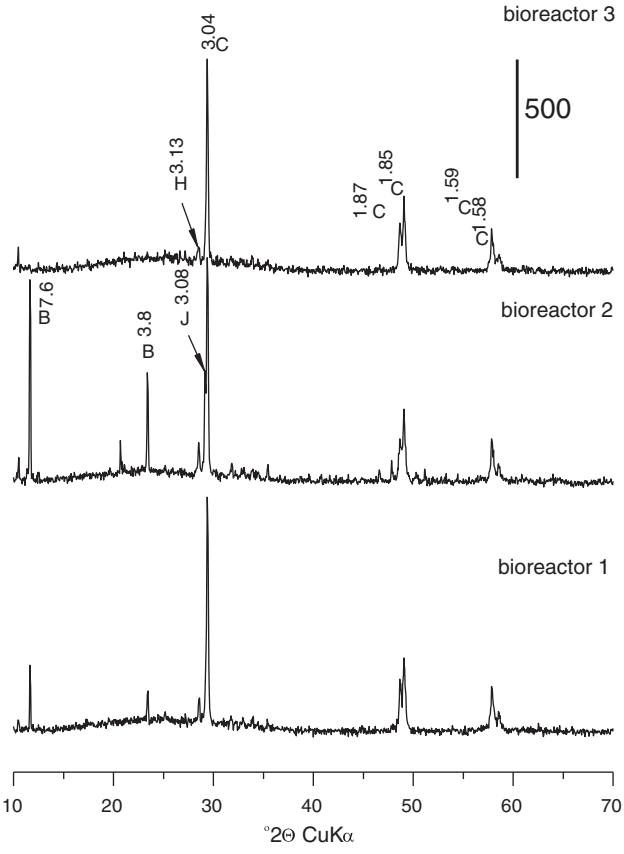

Fig. 12. X-ray diffractograms of solid residues from bioreactors after 34 days of leaching. Bioreactor 1: *A. ferrooxidans* followed by 100 mM Na-chloride addition on day 15; bioreactor 2: *A. ferrooxidans* and 100 mM Na-chloride followed by addition of *A. thiooxidans* inoculum on day 9; bioreactor 3: 100 mM Na-chloride followed by addition of *A. ferrooxidans* inoculum on day 15. Letter designations: B = brushite, C = chalcopyrite, H = hornblende, and J = jarosite. The vertical bar shows the relative scale of counts. The *d*-values are given in Ångströms.

In contrast, only chalcopyrite and hornblende were detected in solids after 14 days of contact with *A. ferrooxidans* and 100 mM Na-chloride in shake flasks (Fig. 9). The second intense peak ($d = 2.71$) is assigned to silica wafer in the sample holder, which was not completely full with the sample material. Neither S^0 nor secondary Cu-sulfides (e.g., Cu or Cu_2S) were detected with XRD in solid residues in these experiments (Figs. 8 and 9). They were also undetectable after 15 days of contact with 100 mM Na-chloride and the mixture of *A. ferrooxidans* and *A. thiooxidans* (data not shown). XRD analysis of solid residues after 42 days of contact in abiotic controls ± Na-chloride showed that these samples were free of any secondary phases (data not shown), indicating that the formation of solid phase reaction products was of minor significance.

X-ray diffractograms of solids from two *A. ferrooxidans* cultures sampled on day 58 are compared in Fig. 10. Both suspensions were re-inoculated on day 44, at which time one culture also received 100 mM Na-chloride. Solids from the culture without Na-chloride contained brushite, gypsum, and jarosite as major secondary phases. In the parallel Na-chloride-supplied culture the secondary solid phases were relatively less abundant. The peak at $d = 3.13$ Å is assigned to hornblende but may also mask a minor amount of a jarosite type precipitate.

After 58 days of contact with *A. ferrooxidans* culture and 100 mM Na-chloride (with *A. thiooxidans* added on day 15), secondary phases were not detected in residual solids (Fig. 11). Quartz was relatively enriched and minor peaks were detected for hydroxylapatite and hornblende. The lack of secondary phases in the residual solids indicated that sulfur compounds and ferric iron remained in solution with 100 mM Na-chloride. Under more oxidizing conditions (Set 9, spent *A. ferrooxidans* medium with bacteria and 100 mM Na-chloride), the jarosite peaks were pronounced and brushite was also present. In other 58 day solids, jarosite in *A. ferrooxidans* cultures was below the level of XRD detection with 100 mM Na-chloride, and none of the samples contained elemental S or secondary Cu-sulfides (data not shown).

Residual solids from the bioreactor runs after 34 days of operation were also characterized by XRD. In run 1, solids contained residual chalcopyrite and hornblende, and brushite and a jarosite type mineral were detected as secondary phases (Fig. 12). Similarly, these phases

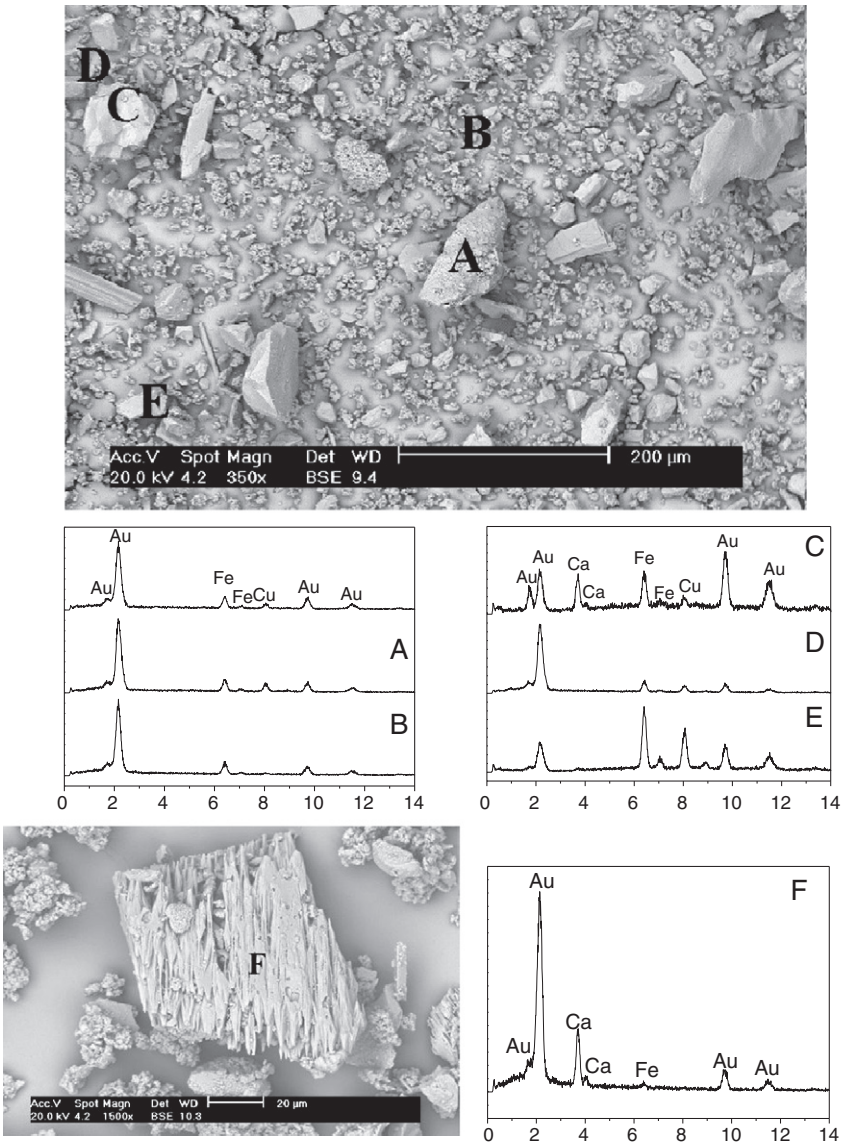

Fig. 13. General outline of SEM-EDXS analyses of solid residues from shake flask chalcopyrite experiments. The letters A, B, C, D, E and F in the SEM micrographs indicate the different types of solids that were analyzed by EDXS. The unlabeled EDS pattern is the blank without a specimen. Detailed results for 22 samples are summarized in Table 3.

were detected in solids from run 2. Neither brushite nor jarosite peaks could be resolved in X-ray diffractograms for residual solids from run 3.

3.4. Energy dispersive X-ray spectroscopy (EDXS)

Fig. 13 shows SEM micrographs of solid residues from shake-flask experiments in inoculated MSM (no Na-chloride) and the corresponding EDXS spectra. The data for spot analyses of different types of precipitates, particles and corroded/pitted regions are summarized in Table 3.

In general, particle surfaces were relatively clean in the SEM micrographs. In few instances, the particles displayed corroded appearance and coatings with precipitates that could represent jarosites, brushite or other secondary phases. Secondary, Fe-deficient Cu-sulfides and S^0, if present, were below the detection level by XRD. The presence of P in the precipitates was also noted, and may be in keeping with brushite detected in X-ray diffractograms, or unreacted hydroxylapatite present in the original sample. Ca and P containing phases displayed increased weathering in the presence of Na-chloride. In order to confirm the chemical nature of different features observed on the residues, EDXS microanalysis was performed at representative (magnification 350×, EDXS numbers 1, 6, 12 and 19) and spot areas (Table 3). The other EDXS numbers (Table 3) correspond to the composition of the different regions analyzed for each sample.

In sample 1 residues of Set 8 (MSM, no bacteria and no Na-chloride), no major change was noticed for the appearance of chalcopyrite surfaces; Ca- and P-containing particles showed signs of corrosion; P-, S- and Fe-containing precipitates were aggregated on some particle surfaces. In sample 2 residues of Set 7 (MSM with Na-chloride, no bacteria), Ca- and P-containing particles were extensively corroded and there were P-, S- and Fe-containing precipitates on some particle surfaces. In sample 3 residues of Set 5 (MSM, with bacteria, no Na-chloride), P was not found in solids, whereas S- and Fe-containing precipitates were detected. Ca was also detected, suggesting the presence of gypsum; chalcopyrite surface did not show much corrosion or pitting as expected due to its refractory nature in the bioleaching. In sample 4 residues of Set 1 (MSM with bacteria and Na-chloride), Si was detected in some corroded particles (and Mg in one sample), suggesting the presence of silicate phase(s) (possibly quartz or hornblende) in the concentrate; Ca- and P-containing particles showed extensive corrosion; chalcopyrite surfaces did not show much corrosion or pitting; and Fe- and S-containing precipitates were detected on mineral grains, ascribed to jarosites.

3.5. Electrochemical characterization of solid residues

Electrochemical impedance spectroscopy (EIS), as used in this work, is related to the behavior of the electrode surface/solution interface only and it was chosen to better resolve changes on the mineral surface under different bioleaching conditions. It involved applying small AC potential perturbation on the open circuit potential or on desired DC potential by varying the frequency and recording certain number of points/frequency decade.

A CPE in MSM without Fe^{2+}, S^0, or chalcopyrite showed a phase angle near −90° in a large frequency range (300–0.01 Hz) and modulus of impedance values around 10^7 Ω. A CPE with 20 wt.% chalcopyrite showed a phase angle near −65° at around 10 Hz and the corresponding modulus of impedance was around 10^4–10^5 Ω cm^2, at least two orders of magnitude lower that the CPE graphite because chalcopyrite, by comparison to graphite, is more readily oxidized in the electrochemical system (Horta et al., 2009). EIS measurements are difficult to perform during the bioleaching because electrochemically active minerals are suspended in solution and not fixed to the electrode surface. Therefore, EIS measurements were carried out with solid residues from selected bioleaching experiments to characterize their impedance behavior.

Fig. 14 shows the EIS diagrams obtained for the abiotic control (Set 8, Control, Table 1). At least two time constants were observed, one with a phase angle around −70° centered at 56 Hz, and the other was not well-defined at frequencies <0.1 Hz. The modulus of impedance was around 300 kΩ after 14 days and decreased by one order of magnitude after 28 days of leaching. This resistive behavior matched with the Nyquist plots. After 28 days the EIS signal stabilized and no further differences were observed for solids that had been leached for 42 d. The modulus of impedance was much higher than that determined for the CPE-chalcopyrite and the phase angle value

Table 3
EDXS analysis of solid residues from shake flask chalcopyrite leaching experiments. The outline of the SEM/EDXS analyses is illustrated in Fig. 13.

Experimental condition	EDXS no.	SEM-EDXS analysis (wt.%)					XRD summary of solid phases identified in the Set
		S	Fe	P	Cu	Ca	
MSM only (no Na-chloride, no bacteria) Designation: Control (Set 8, Table 1)	1	5.47	8.18	2.33	6.98	0.76	Chalcopyrite, hornblende, hydroxylapatite
	2	12.3	12.7	1.29	14.9	nd	
	3	nd[a]	1.92	10.1	nd	20.1	
	4	11.8	24.6	5.52	17.9	0.99	
	5	9.36	9.97	3.61	8.97	nd	
MSM with 100 mM Na-chloride Designation: Cl (Set 7, Table 1)	6	5.33	8.80	nd	6.55	nd	Chalcopyrite, hornblende, hydroxylapatite
	7	nd	4.14	nd	1.72	5.44	
	8	5.86	22.5	nd	9.54	nd	
	9	2.19	7.66	nd	9.48	nd	
	10	nd	2.09	7.60	1.50	12.2	
	11	1.45	1.92	7.17	1.98	9.60	
MSM + CuFeS2-adapted *A. ferrooxidans*, no Na-chloride Designation: Af (Set 5, Table 1)	12	4.35	9.51	nd	5.72	0.68	Chalcopyrite, hornblende, brushite, gypsum, jarosite
	13	2.12	12.6	nd	2.87	nd	
	14	6.95	10.2	nd	11.6	nd	
	15	0.78	5.84	nd	2.94	3.20	
	16	1.48	16.0	nd	18.7	0.36	
	17	7.27	9.52	nd	10.4	nd	
	18	6.14	9.51	nd	7.37	nd	
MSM + *A. ferrooxidans* + 100 mM Na-chloride Designation: Cl + *Af* (Set 1, Table 1)	19	7.07	13. 7	2.80	1.17	9.09	Chalcopyrite, hornblende, brushite, gypsum, jarosite
	20	0.68	11.1	0.84	nd	14.9	Some solids contained 5.73% Mg and 1.38–2.89% Si
	21	1.76	14.3	2.54	8.65	1.66	
	22	0.45	15.4	2.35	nd	nd	
	23	1.70	5.29	4.91	nd	2.99	
	24	11.3	9.44	2.59	nd	10.7	
	25	1.50	3.23	6.12	7.09	2.59	

[a] nd, not detected.

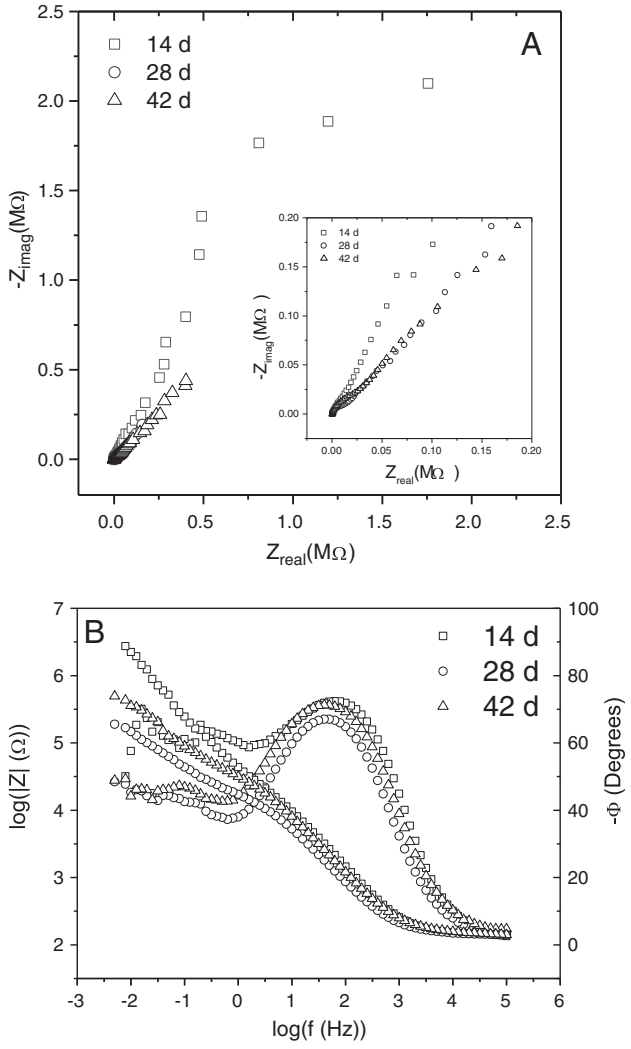

Fig. 14. Impedance diagrams of (A) Nyquist and (B) Bode phase angle, −Φ and log|Z| vs. log f, determined for solid residues from the abiotic chalcopyrite control (Set 8, Control, Table 1). The geometric area exposed to the solution was 7.1 mm^2.

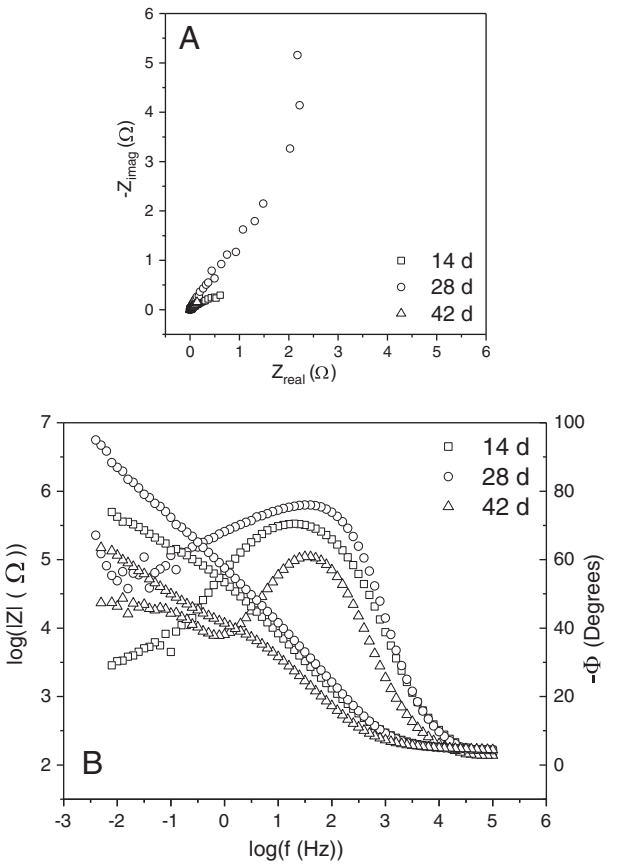

Fig. 15. Impedance diagrams of (A) Nyquist and (B) Bode phase angle, −Φ and log|Z| vs. log f, determined for solid residues from the abiotic chalcopyrite control leached with 100 mM Na-chloride (Set 7, Cl, Table 1). The geometric area exposed to the solution was 7.1 mm^2.

was the same but shifted to lower frequency, indicating that the residue from the bioleaching was passive as compared to chalcopyrite.

Electrochemical response was also determined for solid residues from the abiotic control that was leached with 100 mM Na-chloride (Set 7, Cl, Table 1). Two time constants were observed, one appearing at higher frequency. For the 14 day sample, the phase angle and the corresponding frequency (Fig. 15B) were almost the same as in the control shown in Fig. 14 (Set 8, Table 1). For the 14 and 28 day samples, the phase angle was increased to about −80° as compared to the control, and the maximum increased indicating an increase in the capacitive behavior. These results are consistent with the formation of less conductive precipitates as a consequence of the pH increase (Fig. 5) and the decrease in the concentration of ferrous and total iron in the solution. All these results suggest the passivation of the chalcopyrite surface. For 42 day samples the behavior was similar to that observed for the control as the other time constant appeared at the low frequency region.

After 14 days of leaching, the phase angle reached 30°, while with the 28 and 42 day samples the phase angle increased to about 55° and 45°, respectively, and a higher dispersion was noted which was attributed to the presence of Na-chloride. The higher dispersion in the presence of Na-chloride means that chloride ion disturbs the passive layer by decreasing the precipitation of iron and modifying the XRD-undetectable S^0 layer. In a previous study of CPE-chalcopyrite using electrochemical noise analysis (Horta et al., 2009), high dispersion was observed around zero in the admittance versus time after adding chloride ion to the sample solution. This finding indicated that the system became electrochemically active, whereas in the absence of chloride only a low dispersion around zero was detected in the corresponding admittance time course curves. No dispersion was observed when *A. ferrooxidans* was added to the system in the absence of chloride ion. This response was similar to the passive behavior due to bacterial adhesion on the CPE-chalcopyrite surface (Horta et al., 2009).

Fig. 16 shows the EIS diagrams for solids from *A. ferrooxidans* cultures with residues of Set 5 and without 100 mM Na-chloride, and residues of Set 1 after 14 and 42 days of leaching. All conditions presented at least two time constants as observed before. However, the lowest frequency was not well defined. The presence of bacteria increased the maximum, centering at around 56 Hz. A new time constant centered at 1 Hz for residues of Set 5 (condition 3) was observed. In the presence of Na-chloride and bacteria, the Bode phase angle–frequency curves for residues of Set 1 (condition 4) were comparable with the 14 and 42 day samples of residues of Set 7 (condition 2), although the actual interfacial phenomena may be different. The impedance modulus value at the lowest frequency was the highest for residues of Set 1 condition 4 (42 day sample). The values were the same for the 14 and 42 day residue samples of Set 5 (condition 3) and the 14 day sample of residues of Set 1 (condition 4). For residue samples from Set 8, Set 7, and Set 5 conditions 1 to 3, the impedance modulus values oscillated at low frequencies.

The presence of a new time constant at middle frequency in inoculated experiments is attributed to the formation of secondary phases (at least brushite and jarosite) and bacterial biofilm. The residue from these treatments should be more stable and thus be less subject to

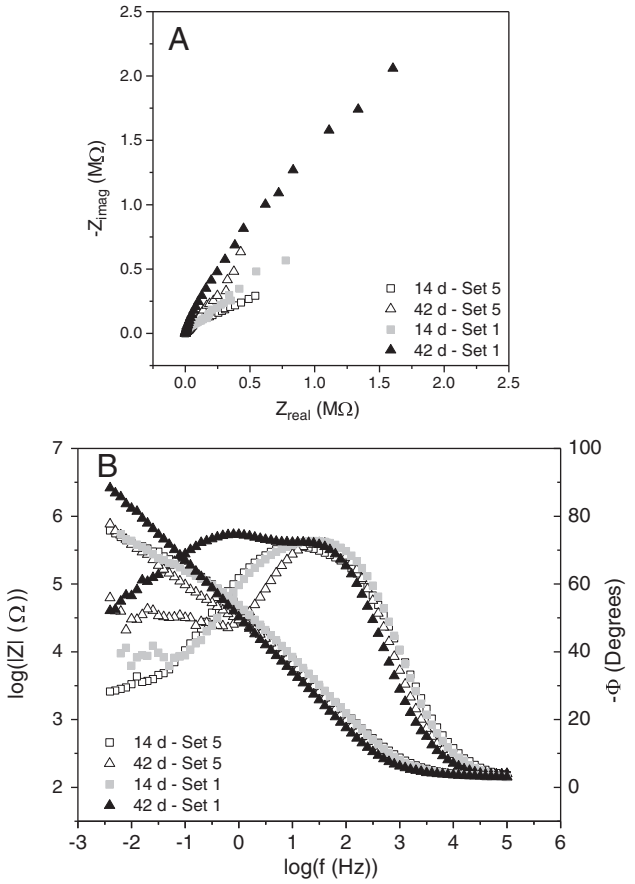

Fig. 16. Impedance diagrams of (A) Nyquist and (B) Bode phase angle, $-\Phi$ and log|Z| vs. log f, determined for solid residues from inoculated chalcopyrite leaching experiments (Set 1, Cl + *Af*; Set 5, *Af*; Table 1). The geometric area exposed to the solution was 7.1 mm^2.

dispersion at low frequencies. The influence of the presence of bacteria is more evident based on real impedance versus frequency plots (Fig. 17). The effect of bacteria in the presence and absence of Na-chloride was also observed at the high frequency region. No difference in impedance was observed in the absence of bacteria (Fig. 16). The combined action of bacteria and Na-chloride suggested that the leaching process was not stabilized even after 42 days, as indicated by the linear response of real impedance versus frequency (Fig. 17) at low frequency region.

4. Discussion

The dissolved Fe concentration was about 120 mM in *A. ferrooxidans* cultures, mostly as Fe^{3+} due to bacterial oxidation of iron. Jarosite precipitation varied depending on the contact time and the presence of Na-chloride. The addition of 100 mM Na-chloride to cultures minimized jarosite precipitation, and the concentration of dissolved Fe increased with time when jarosite was only a relatively minor phase. Secondary Cu-sulfides and S^0 were not found in the solid residues by XRD. However, secondary Cu-sulfides form during chalcopyrite bioleaching (Ahmadi et al., 2011; He et al., 2012; Xia et al., 2010) and, for example, intermediate chalcocite and covellite, possibly also talnakhite ($Cu_9(Fe,Ni)_8S_{16}$) and bornite (Cu_5FeS_4), have been demonstrated by cyclic voltammetry of chalcopyrite electrode (Qin et al., 2013). In the present study, the influence of new solid phases such jarosites formed during the leaching reactions could be detected by EIS by comparing the increase in the modulus of impedance and changes in the phase angle values and their frequency values with the untreated chalcopyrite response.

Neither Na-chloride alone nor *A. thiooxidans* improved Cu dissolution from chalcopyrite. Cu dissolution was improved in the presence of 100 mM Na-chloride and *A. ferrooxidans* compared to the bioleaching only with bacteria. The second addition of 100 mM Na-chloride was initially inhibitory to bacterial oxidation of iron, but the culture adapted to

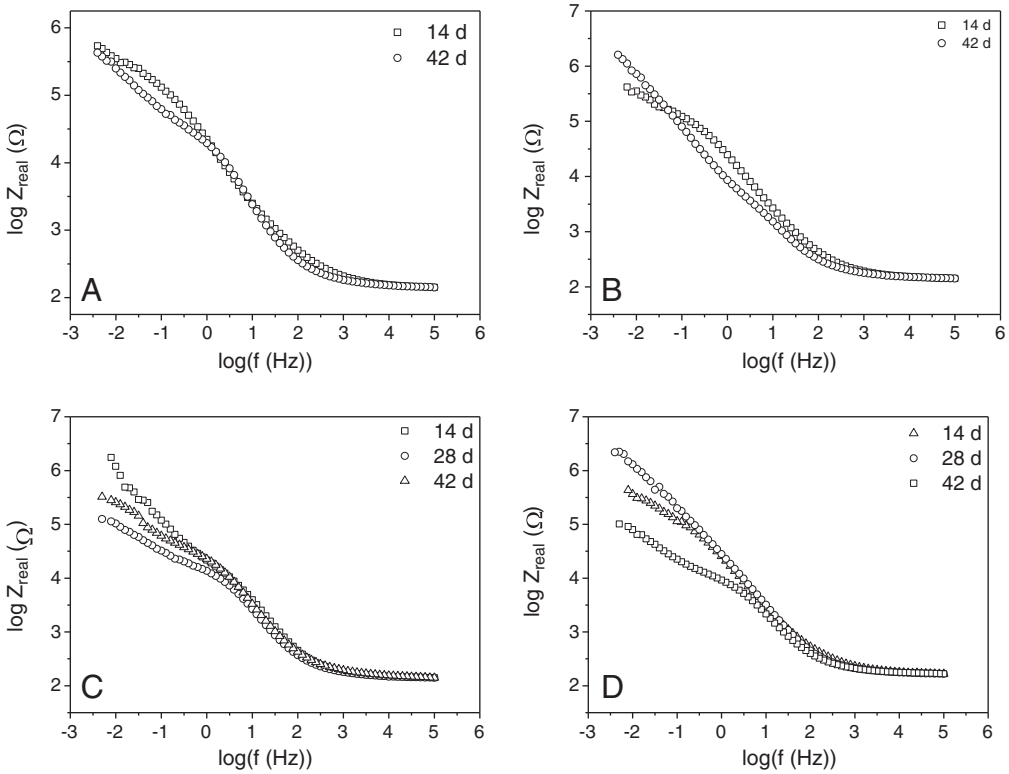

Fig. 17. Impedance versus frequency plots of solid residues from chalcopyrite leaching experiments. A, Set 1 (Cl + *Af*); B, Set 5 (*Af*); C, Set 7 (Cl); D, Set 8 (Control). The geometric area exposed to the solution was 7.1 mm^2.

200 mM Na-chloride concentration within two weeks. The concentration of dissolved Fe increased in inoculated flasks containing100 mM Na-chloride in parallel with redox potential and a decrease in pH. In Na-chloride-containing abiotic controls the pH values increased and iron precipitated, whereas jarosites were not detected in Na-chloride-containing inoculated cultures. The chemical leaching of chalcopyrite was not enhanced with the addition of 100–200 mM Na-chloride.

The two time constants observed in EIS diagrams may be attributed to (i) the semiconductor character of chalcopyrite, with the secondary phases covering the electrode surface (at high frequencies), and (ii) the charge transfer processes at low frequency region involving different electrochemical reactions such as chalcopyrite oxidation, corrosion of mineral particles, and formation of precipitates (brushite and jarosite). The time constant at high frequency is also influenced by the presence of biofilm (Bevilaqua et al., 2004). At the high frequency region the changes in Bode phase angle and impedance modulus are related to the presence of different solid phase products formed during the bioleaching. These products (brushite and jarosite) accumulate on chalcopyrite surface leading to the modification of impedance diagram when compared with pure chalcopyrite. For instance, the modulus of impedance of CPE-(20 wt.%) chalcopyrite is about 30 kΩ (Bevilaqua et al., 2011), while the solid residues from different experimental conditions of bioleaching showed impedance modulus values at least one order of magnitude higher. Jarosite and bacterial attachment in the inoculated experiments may be responsible for the new time constant at middle frequency. This signal may also be interpreted to involve extracellular polymeric materials produced by iron-oxidizing bacteria under bioleaching conditions (Gehrke et al., 1998; Rohwerder and Sand, 2007; Sand and Gehrke, 2006; Skłodowska and Matlakowska, 1998).

Mixed Cu and Fe oxides may also form on mineral surfaces due to the exposure to air, and they can decrease the conductive nature of the electrode. In acidic media oxide layers on mineral surfaces are removed by acid attack, which may contribute to low but continuous copper dissolution seen in time course graphs. Analysis of impedance with high frequency also demonstrated that bacteria influenced the oxidation both in the presence and absence of Na-chloride. Mineral surface oxidation was not observed in the absence of bacteria. The differences can be attributed to bacterial enhancement of mineral surface oxidation and chloride modification of dissolution and precipitation products. These two processes result in a combined effect, which may be responsible for the continuing leaching process even after 42 d, as indicated by the response at low frequency region.

5. Conclusions

Na-chloride at 100 mM concentration did not affect the chemical leaching of copper from chalcopyrite. The dissolution was enhanced in the presence of 100 mM Na-chloride and *A. ferrooxidans* compared to leaching with *A. ferrooxidans* without Na-chloride. S^0 was not detected during chalcopyrite leaching in the presence of 100 mM Na-chloride and *A. ferrooxidans*. Fe(III) precipitates were not detected under these conditions either, except when a spent culture of *A. ferrooxidans* containing 120 mM Fe^{3+} was used. As corroborated by EIS analyses, the combined action of bacteria and Na-chloride suggested a synergistic effect on chalcopyrite dissolution because the leaching process continued even after 42 days of contact time. It is evident that EIS is a good tool to demonstrate the influence of new phases formed during leaching and bioleaching of minerals by analysis of their residues.

Acknowledgments

This research was funded by the Finnish Funding Agency for Technology and Innovation (Finland Distinguished Professor Program, 402/06). Additional support for this study was received from CNPq (AVB, 305890/2010-7) and Vale SA (Brazil). We thank F.S. Jones (School of Environment and Natural Resources, Ohio State University) for the expert input in XRD data interpretation and two anonymous reviewers for insightful comments and input that were helpful in improving the manuscript.

References

Ahmadi, A., Schaffie, M., Petersen, J., Schippers, A., Ranjbar, M., 2011. Conventional and electrochemical bioleaching of chalcopyrite concentrates by moderately thermophilic bacteria at high pulp density. Hydrometallurgy 106, 84–92.

Al-Harahsheh, M., Kingman, S., Al-Harahsheh, A., 2008. Ferric chloride leaching of chalcopyrite: synergetic effect of $CuCl_2$. Hydrometallurgy 91, 89–97.

American Public Health Association; American Water Works Association; Water Environment Federation, 1998. Standards Methods for the Examination of Water and Wastewater, 20th ed. American Public Health Association, Washington, D.C.

Bevilaqua, D., Leite, A.L.L.L., Garcia Jr., O., Tuovinen, O.H., 2002. Oxidation of chalcopyrite by *Acidithiobacillus ferrooxidans* and *Acidithiobacillus thiooxidans* in shake flasks. Process. Biochem. 38, 589–594.

Bevilaqua, D., Diez-Perez, I., Fugivara, C.S., Sanz, F., Benedetti, A.V., Garcia Jr., O., 2004. Oxidative dissolution of chalcopyrite ($CuFeS_2$) by *Acidithiobacillus ferrooxidans* analyzed by electrochemical impedance spectroscopy and atomic force microscopy. Bioelectrochemistry 64, 79–84.

Bevilaqua, D., Acciari, H.A., Arena, F.A., Benedetti, A.V., Fugivara, C.S., Filho, G.T., Garcia Jr., O., 2009. Utilization of electrochemical impedance spectroscopy for monitoring bornite (Cu_5FeS_4) oxidation by *Acidithiobacillus ferrooxidans*. Miner. Eng. 22, 254–262.

Bevilaqua, D., Suegama, P.H., Garcia Jr., O., Benedetti, A.V., 2011. Electrochemical studies of sulphide minerals in the presence and absence of *A. ferrooxidans*. In biohydrometallurgical processes: a practical approach. In: Sobral, L.G.S., de Oliveira, D.M., de Souza, C.E.G. (Eds.), Centro de Tecnologia Mineral, Ministry of Science, Education and Innovation, Rio de Janeiro, pp. 141–167.

Cai, Y., Chen, X., Ding, J., Zhou, D., 2012. Leaching mechanism for chalcopyrite in hydrochloric acid. Hydrometallurgy 113–114, 109–118.

Carneiro, M.F.C., Leão, V.A., 2007. The role of sodium chloride on surface properties of chalcopyrite leached with ferric sulfate. Hydrometallurgy 87, 73–82.

Davis-Belmar, C.S., Nicolle, J.L.C., Norris, P.R., 2008. Ferrous iron oxidation and leaching of copper ore with halotolerant bacteria in ore columns. Hydrometallurgy 94, 144–147.

Deveci, H., Jordan, M.A., Powell, N., Alp, I., 2008. Effect of salinity and acidity on bioleaching activity of mesophilic and extremely thermophilic bacteria. Trans. Nonferrous Met. Soc. China 18, 714–721.

Dopson, M., Lindström, E.B., 1999. Potential role of *Thiobacillus caldus* in arsenopyrite bioleaching. Appl. Environ. Microbiol. 65, 36–40.

Fu, B., Zhou, H., Zhang, R., Qiu, G., 2008. Bioleaching of chalcopyrite by pure and mixed cultures of *Acidithiobacillus* spp. and *Leptospirillum ferriphilum*. Int. Biodeterior. Biodegrad. 62, 109–115.

Gahan, C.S., Sundkvist, J.-E., Sandström, Å., 2009. A study on the toxic effects of chloride on the biooxidation efficiency of pyrite. J. Hazard. Mater. 172, 1273–1281.

Gahan, C.S., Sundkvist, J.-E., Dopson, M., Sandström, Å., 2010. Effect chloride on ferrous iron oxidation *Leptospirillum ferriphilum*-dominated chemostat culture. Biotechnol. Bioeng. 106, 422–431.

Garcia Jr., O., 1991. Isolation and purification of *Thiobacillus ferrooxidans* and *Thiobacillus thiooxidans* from some Brazilian uranium mines. Rev. Microbiol. 22, 1–6.

Gerhke, A., Telegdi, J., Thierry, D., Sand, W., 1998. Importance of extracellular polymeric substances from *Thiobacillus ferrooxidans* for bioleaching. Appl. Environ. Microbiol. 64, 2743–2747.

Harahuc, L., Lizama, H.M., Suzuki, I., 2000. Selective inhibition of the oxidation of ferrous iron or sulfur in *Thiobacillus ferrooxidans*. Appl. Environ. Microbiol. 66, 1031–1037.

He, H., Xia, J.-L., Yang, Y., Jiang, H., Xiao, C.-Q., Zheng, L., Ma, C.Y., Zhao, Y.-D., Qiu, G.-Z., 2009. Sulfur speciation on the surface of chalcopyrite leached by *Acidianus manzaensis*. Hydrometallurgy 99, 45–50.

He, H., Xia, J.-L., Hing, F.-F., Tao, X.-X., Leng, Y.-W., Zhao, Y.-D., 2012. Analysis of sulfur speciation on chalcopyrite surface bioleached with *Acidithiobacillus ferrooxidans*. Miner. Eng. 27–28, 60–64.

Horta, D.G., Bevilaqua, D., Acciari, H.A., Garcia Jr., O., Benedetti, A.V., 2009. Optimization of the use of carbon paste electrodes (CPE) for electrochemical study of the chalcopyrite. Quím. Nova 32, 1734–1738.

Kaksonen, A.H., Lavonen, L., Kuusenaho, M., Kolli, A., Närhi, H., Vestola, E., Puhakka, J.A., Tuovinen, O.H., 2011. Bioleaching and recovery of metals from final slag waste of the copper smelting industry. Miner. Eng. 24, 1113–1121.

Kinnunen, P.H.-M., Puhakka, J.A., 2004. Chloride promoted leaching of chalcopyrite concentrate by biologically-produced ferric sulfate. J. Chem. Technol. Biotechnol. 79, 830–834.

Klauber, C., 2008. A critical review of the surface chemistry of acidic ferric sulphate dissolution of chalcopyrite with regards to hindered dissolution. Int. J. Miner. Process. 86 (1–4), 1–17.

Liang, C.-L., Xia, J.-L., Nie, Z.-Y., Yang, Y., Ma, C.-Y., 2012. Effect of sodium chloride on sulfur speciation of chalcopyrite bioleached by the extreme thermophile *Acidianus manzaensis*. Bioresour. Technol. 110, 462–467.

Lu, Z.Y., Jeffrey, M.I., Lawson, F., 2000. The effect of chloride ions on the dissolution of chalcopyrite in acidic solutions. Hydrometallurgy 56, 189–202.

Mansfeld, F., Lin, S., Chen, Y.C., Shin, H., 1988. Minimization of high-frequency phase shifts in impedance measurements. J. Electrochem. Soc. 135, 906–907.

Panda, S., Parhi, P.K., Nayak, B.D., Pradhan, N., Mohapatra, U.B., Sukla, L.B., 2013. Two step meso-acidophilic bioleaching of chalcopyrite containing ball mill spillage and removal of the surface passivation layer. Bioresour. Technol. 130, 332–338.

Qin, W., Yang, C., Lai, S., Wang, J., Liu, K., Zhang, B., 2013. Bioleaching of chalcopyrite by moderately thermophilic microorganisms. Bioresour. Technol. 129, 200–208.

Rodríguez, Y., Ballester, A., Blázquez, M.L., González, F., Munoz, J.A., 2003. New information on the chalcopyrite bioleaching mechanism at low and high temperature. Hydrometallurgy 71, 47–56.

Rohwerder, T., Sand, W., 2007. Mechanisms and biochemical fundamentals of bacterial metal sulfide oxidation. In: Donati, E.R., Sand, W. (Eds.), In Microbial Processing of Metal Sulfides. Springer Verlag, Berlin, pp. 35–58.

Ruiz, M.C., Montes, K.S., Padilla, R., 2012. Chalcopyrite leaching in sulfate-chloride media at ambient pressure. Hydrometallurgy 109, 37–42.

Sand, W., Gehrke, T., 2006. Extracellular polymeric substances mediate bioleaching/biocorrosion via interfacial processes involving iron(III) ions and acidophilic bacteria. Res. Microbiol. 157, 49–56.

Sasaki, K., Nakamuta, Y., Hirajima, T., Tuovinen, O.H., 2009. Raman characterization of secondary minerals formed during chalcopyrite leaching with *Acidithiobacillus ferrooxidans*. Hydrometallurgy 95, 153–158.

Sato, H., Nakazawa, H., Kudo, Y., 2000. Effect of silver chloride on the bioleaching of chalcopyrite concentrate. Int. J. Miner. Process. 59, 17–24.

Shiers, D.W., Blight, K.R., Ralph, D.E., 2005. Sodium sulphate and sodium chloride effects on batch culture of iron-oxidizing bacteria. Hydrometallurgy 80, 75–82.

Skłodowska, A., Matlakowska, R., 1998. Relative surface charge, hydrophobicity of bacterial cells and their affinity to substrate during copper bioleaching from post-flotation wastes. Biotechnol. Lett. 20, 229–333.

Tuovinen, O.H., Kelly, D.P., 1973. Studies on the growth of *Thiobacillus ferrooxidans*. I. Use of membrane filters and ferrous iron agar to determine viable numbers, and comparison with $^{14}CO_2$-fixation and iron oxidation as measures of growth. Arch. Mikrobiol. 88, 285–298.

Wang, Y., Su, L., Zhang, L., Zeng, W., Wu, J., Wan, L., Qiu, G., Chen, X., Zhou, H., 2012. Bioleaching of chalcopyrite by defined mixed moderately thermophilic consortium including a marine acidophilic halotolerant bacterium. Bioresour. Technol. 121, 348–354.

Watling, H.R., 2006. The bioleaching of sulphide minerals with emphasis on copper sulphides — a review. Hydrometallurgy 84, 81–108.

Xia, J.-L., Yang, Y., He, H., Liang, C.-L., Zhao, X.-J., Zheng, L., Ma, C.-Y., Zhao, Y.-D., Nie, Z.-Y., Qiu, G.-Z., 2010. Investigation of the sulfur speciation during chalcopyrite leaching by moderate thermophile *Sulfobacillus thermosulfidooxidans*. Int. J. Miner. Process. 94, 52–57.

Xiong, H., Guo, R., 2011. Effects of chloride acclimation on iron oxyhydroxides and cell morphology during cultivation of *Acidithiobacillus ferrooxidans*. Environ. Sci. Technol. 45, 235–240.

Yoo, K., Kim, S.-K., Lee, J.-C., Ito, M., Tsunekawa, M., Hiroyoshi, N., 2010. Effect of chloride ions on leaching rate of chalcopyrite. Miner. Eng. 23, 471–477.

Zammit, C.M., Mangold, S., Rao Jonna, V., Mutch, L.A., Watling, H.R., Dopson, M., Watkin, E.L.J., 2012. Bioleaching in brackish waters — effect of chloride ions on the acidophile population and proteomes of model species. Appl. Microbiol. Biotechnol. 93, 319–329.

Zeng, W., Qiu, G., Chen, M., 2013. Investigation of Cu–S intermediate species during electrochemical dissolution and bioleaching of chalcopyrite concentrate. Hydrometallurgy 134–135, 158–165.

Zhou, Q.G., Bo, F., Bo, Z.H., Xi, L., Jian, G., Fei, L., Hua, C., 2007. Isolation of a strain of *Acidithiobacillus caldus* and its role in bioleaching of chalcopyrite. World J. Microbiol. Biotechnol. 23, 1217–1225.